

Donor and acceptor states in lightly doped polyacetylene, $(\text{CH})_x$

C. R. Fincher, Jr., M. Ozaki,* A. J. Heeger, and A. G. MacDiarmid

Laboratory for Research on the Structure of Matter, University of Pennsylvania, Philadelphia, Pennsylvania 19104

(Received 29 November 1978)

The results of an experimental study of the infrared absorption of the $(\text{CH})_x$ system, lightly doped ($< 0.1\%$) with acceptors and donors, are presented. Additional absorptions are observed near 1370 cm^{-1} (width $\sim 50\text{ cm}^{-1}$) and 900 cm^{-1} (width $\sim 400\text{ cm}^{-1}$) upon doping with iodine, AsF_5 , and sodium. The two additional absorption maxima appear to be general features of lightly doped $(\text{CH})_x$ independent of specific dopant or of *cis* (*trans*) content. Measurements on stretch-oriented films demonstrate that these absorption maxima are polarized primarily along the polymer chains. The narrow mode at 1370 cm^{-1} is attributed to a molecular vibration made ir active by the doping. The broader absorption centered at 900 cm^{-1} is discussed in terms of quasi-one-dimensional donor and acceptor bound states along the $(\text{CH})_x$ chain. We include an experimental determination of the room-temperature dielectric constant in undoped $(\text{CH})_x$; $\epsilon_{\parallel} \approx 10\text{--}12$, with uncertainty arising from the incomplete orientation of the $(\text{CH})_x$ films. The bound-state energy is thus consistent with a one-dimensional hydrogenic model in which the Coulomb potential along the chain is reduced by ϵ_{\parallel} . Alternatively viewing semiconducting $(\text{CH})_x$ as a Peierls distorted one-dimensional metal, we discuss localized domain-wall-like charged donor (acceptor) states induced by charge-transfer doping.

I. INTRODUCTION

Polyacetylene, $(\text{CH})_x$, is the simplest linear conjugated polymer. Interest in this semiconducting polymer has been stimulated by the successful demonstration of doping with associated control of electrical properties over a wide range^{1,2}; the electrical conductivity of films of $(\text{CH})_x$ can be varied over 12 orders of magnitude from that of an insulator ($\sigma \sim 10^{-9}\ \Omega^{-1}\text{ cm}^{-1}$) through semiconductor to a metal ($\sigma \approx 10^3\ \Omega^{-1}\text{ cm}^{-1}$).³⁻⁵ Various electron donating or accepting molecules can be used to yield *n*-type or *p*-type material, and compensation and junction formation have been demonstrated.⁶ Optical-absorption studies indicate a direct-band-gap semiconductor with a peak absorption coefficient of about $3 \times 10^5\text{ cm}^{-1}$ at 1.9 eV.⁷ Partial orientation of the polymer fibrils by stretch elongation of the $(\text{CH})_x$ films results in anisotropic electrical⁴ and optical⁷ properties suggestive of a highly anisotropic band structure.⁸ The electrical conductivity of partially oriented metallic $[\text{CH}(\text{AsF}_5)_{0.1}]_x$ is in excess of $2000\ \Omega^{-1}\text{ cm}^{-1}$.⁴ The qualitative change in electrical and optical properties at dopant concentrations above a few percent have been interpreted^{3,5} as a semiconductor-metal transition by analogy to that observed in studies of heavily doped silicon.

Although it is clear from Raman studies^{9,10} that charge transfer is involved in the doping process, the nature of the donor and acceptor states in this semiconducting polymer has not been studied in detail. In order to understand the conduction processes and the evolution from an array of isolated impurity centers to a system exhibiting metallic conduction, a thorough investigation of the impur-

ity donor or acceptor states is necessary.

In this paper we present an infrared study of the $(\text{CH})_x$ system lightly doped ($< 0.1\%$) with acceptors and donors. We noted previously¹¹ that additional absorption appears around 0.1 eV with iodine. These measurements have now been expanded to include AsF_5 and Na; the 0.1-eV absorption appears to be a general feature. In addition, a second molecularlike narrow mode is observed at 1370 cm^{-1} on doping. The ability to achieve partial fibril orientation through stretch elongation¹² has made possible polarized transmission measurements with the conclusion that the additional absorptions are polarized primarily parallel to the polymer chains. The experimental results are discussed in terms of donor and acceptor bound states along the $(\text{CH})_x$ chains. Since a description of extended states in semiconductors involves an effective-medium approach, we include an experimental determination of the room-temperature dielectric constant in undoped polyacetylene. The experimental techniques are described in Sec. II, and the results in Sec. III. The data are discussed and analyzed in Sec. IV in terms of a quasi-one-dimensional hydrogenic model of the donor (acceptor) state.

II. EXPERIMENTAL TECHNIQUES

Polyacetylene crystalline films were prepared using techniques similar to those developed by Shirakawa and collaborators¹³ in the presence of a Ziegler catalyst with polymerization carried out at -78°C . X-ray diffraction and scanning-electron-micrograph studies show that films of any *cis* and *trans* composition are polycrystalline and consist

of matted fibrils. As described by Shirakawa *et al.*,¹³ the measured density is 0.4 g/cm³, compared with 1.2 g/cm³ as obtained by flotation techniques, indicating that the polymer fibrils fill only about one third of the film volume. This is shown clearly in electron micrographs obtained in our laboratory, in agreement with the earlier studies.¹³ Samples used in this study were either ~90% *cis* (as grown at -78°C) or 95%–98% *trans* (after thermal isomerization for 2 h at 200°C). Typical polymer films were 60 μm (0.06 mm) in thickness. Orientation was achieved by stretching *cis*-(CH)_x films at room temperature with subsequent additional stretching during isomerization at 200°C. Details on the orientation techniques are presented elsewhere.^{12,14}

Infrared transmission measurements were carried out using both as-grown and oriented films with varying light levels of doping. Doping techniques are described in earlier publications.¹⁻⁵ The maximum doping levels used in these experiments were 0.1 mole% (~1.8 × 10¹⁹ cm⁻³) as determined by weight change of the sample. Lighter levels of doping were monitored by measurement of the electrical conductivity. The dopant concentrations appropriate to Figs. 2, 4, 5, and 6 were obtained by normalizing the measured absorption coefficient to that of the highest concentration (~0.1 mole%). The absolute accuracies on the concentrations are estimated to be ±50%. The ir transmission data were taken with a Perkin-Elmer 225 spectrophotometer equipped with a AgBr polarizer.

Dielectric-constant measurements on undoped (CH)_x were performed using the cavity-perturbation technique of Buravov and Shchegolev¹⁵ at a frequency of 10 GHz. The experimental apparatus has been described in detail in an earlier paper.¹⁶ A long thin rectangular shaped sample consisting of five layers of undoped oriented (CH)_x film (pressed together) was placed at the center of a rectangular transmission TE₁₀₁ cavity. The sample dimensions were such that when the length was perpendicular to the field, the depolarization factor (η) was near unity so the external microwave field is unperturbed. With the long axis of the sample oriented parallel to the field, η was small (~10⁻³), and the internal microwave field induced currents in the sample and thereby perturbed the cavity. Since the losses were found to be negligibly small in the undoped polymer, the dielectric constant could be obtained directly from the shift in cavity frequency,^{15,16}

$$\epsilon_1 - 1 = \frac{1}{\eta} \frac{\delta}{\alpha/\eta - \delta} \approx \frac{\delta}{\alpha}, \quad (1)$$

since $\delta \ll \alpha/\eta$ where $\delta = (f_{\perp} - f_{\parallel})/f_0$ is the fractional

shift and $\alpha = 2V_s/V_c$ is the cavity filling factor (V_s is the sample volume, V_c is the cavity volume). In applying this result to (CH)_x we must recall that because of the fibril nature of the films the density is only one third the theoretical density. Thus the true filling factor is approximately $\frac{1}{3}$ that obtained from the sample volume.

III. EXPERIMENTAL RESULTS

Figure 1 shows a series of curves of the measured transmission through an unoriented film (thickness = 60 μm) at successively higher levels (<0.1 mole%) of the AsF₅ dopant. Two strong infrared absorption features develop in the doped polymer: a narrow mode (width, $\Gamma \approx 50$ cm⁻¹) around 1370 cm⁻¹ and a broad band (width about 400 cm⁻¹) centered around 900 cm⁻¹.

The narrower mode at 1370 cm⁻¹ (Fig. 1) is comparable in width and intensity to other ir-active modes observed in the undoped polymer, suggesting that it arises from a molecular vibration. A comparison of the absorption to the C-H out-of-plane bending mode (1015 cm⁻¹ in the *trans* isomer or 740 cm⁻¹ in the *cis* isomer) indicates that the oscillator strength is quite large. We conclude that doping at a level below 0.1% turns on an ir mode to a strength comparable with the strongest modes of the undoped polymer. The broader absorption near 900 cm⁻¹ (0.1 eV) appears qualitatively different from other modes in the spectrum. The relatively large width distinguishes this absorption from a typical molecular vibration. Figure 2 replots the data of Fig. 1 in terms of the additional absorption over the undoped sample.

The two characteristic absorptions shown in Figs. 1 and 2 for AsF₅-doped (CH)_x appear to be general features of the lightly doped polymer; similar structures are observed for both acceptors and donors including AsF₅, iodine, and Na. For example, Figs. 3 and 4 show the transmission and absorption data obtained from an iodine-doped film

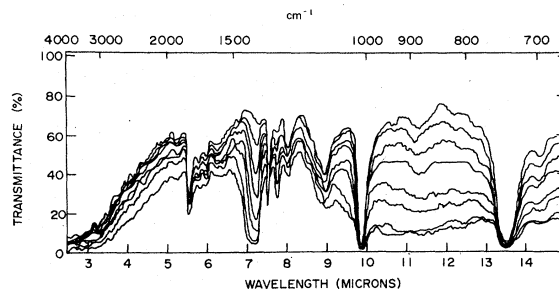


FIG. 1. Transmission through an unoriented film (thickness = 60 μm) of *cis*-(CH)_x at successively higher levels of AsF₅ dopant. The highest dopant concentration corresponds to about 0.1-mole % AsF₅.

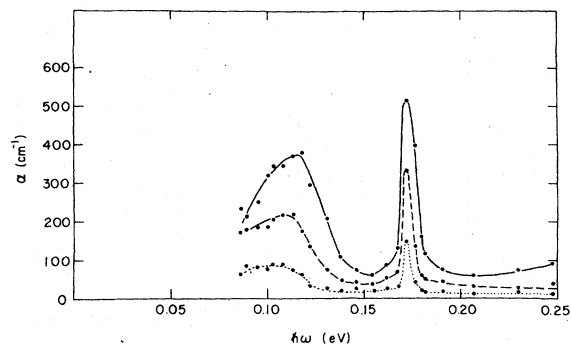


FIG. 2. Additional absorption (over the undoped sample) as a function of energy (in eV) ($<0.1\%$) AsF_5 in $\text{cis}-(\text{CH})_x$. The data were obtained from Fig. 1 (note that $900\text{ cm}^{-1}=0.11\text{ eV}$ and $1370\text{ cm}^{-1}=0.17\text{ eV}$). The upper curve corresponds to approximately 0.1-mole % AsF_5 , the other curves to 0.06% and 0.03%, respectively.

at a similar doping level. The experimental curves for the iodine-doped polymer are nearly identical to those obtained with AsF_5 doping. The absorption data obtained after doping with Na ($<0.1\%$) are shown in Fig. 5. The same two features appear; the results for donor and acceptor doping are essentially indistinguishable.

The effect of variations in (*cis trans*) content has also been investigated. Figures 1-5 were obtained using $(\text{CH})_x$ polymerized at -78°C . The ir bands indicate $\sim 90\%$ *cis* content. Figure 6 shows the absorption results obtained after light doping ($<0.1\%$) of a *trans*- $(\text{CH})_x$ film with iodine. The 1350- and

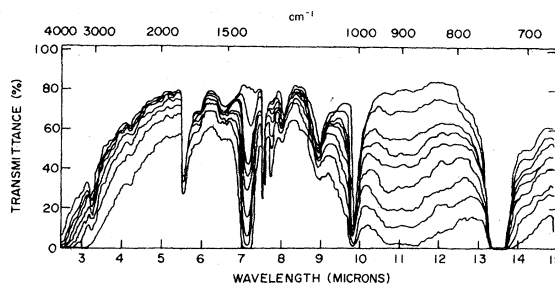


FIG. 3. Transmission through an unoriented film (thickness = $60\text{ }\mu\text{m}$) of $\text{cis}-(\text{CH})_x$ at successively higher levels of iodine dopant. The highest concentration corresponds to about 0.1-mole % iodine.

900-cm^{-1} absorption bands are again clearly evident.

The 900- and 1370-cm^{-1} absorptions are polarized along the polymer chains as demonstrated by the results from oriented films. Figures 7 and 8 show the absorption around 900 and 1370 cm^{-1} for both polarizations, the electric field perpendicular and parallel to the orientation direction. The absorption is much stronger for radiation with the electric field along the chain. It is quite possible that the absorption is entirely polarized and that the observed absorption for the perpendicular polarization is due to the incomplete alignment of the fibrils. As can be seen, the absorption maxima occur at $\hbar\omega_0=0.11\text{ eV}$ with an approximate width of $\hbar\Gamma_0\approx 0.05\text{ eV}$ and $\hbar\omega_1=0.17\text{ eV}$ with an approximate width of $\hbar\Gamma_1\approx 0.005\text{ eV}$. The peak absorption for $\text{CH}(\text{AsF}_5)_{0.001}$ corresponds to an absorption co-

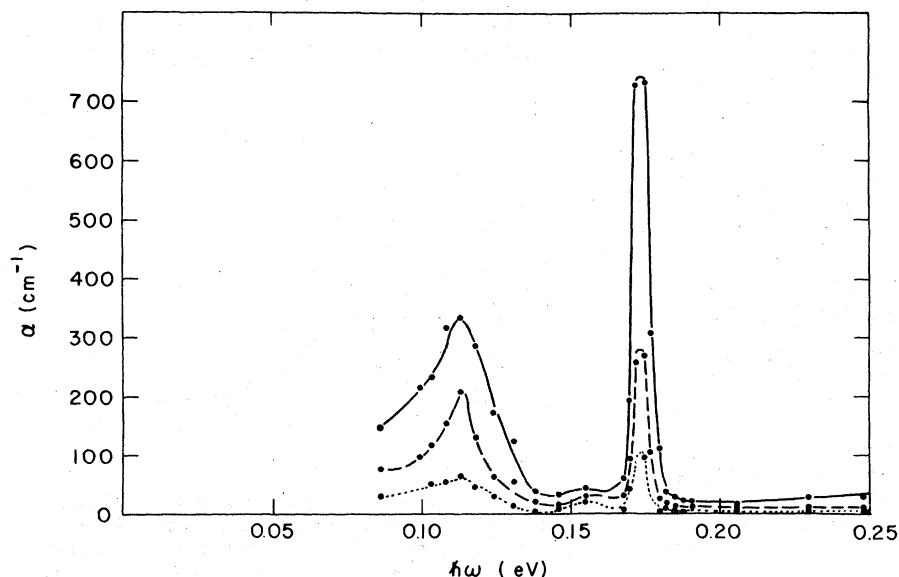


FIG. 4. Additional absorption (over the undoped sample) as a function of energy (in eV) for dilute iodine in $\text{cis}-(\text{CH})_x$. The data were obtained from Fig. 3 (note that $900\text{ cm}^{-1}=0.11\text{ eV}$ and $1370\text{ cm}^{-1}=0.17\text{ eV}$). The upper curve corresponds to approximately 0.1-mole % iodine (or $0.03\% \text{I}_3^-$), the lower curves to 0.05% ($0.016\% \text{I}_3^-$) and 0.015% ($0.005\% \text{I}_3^-$), respectively.

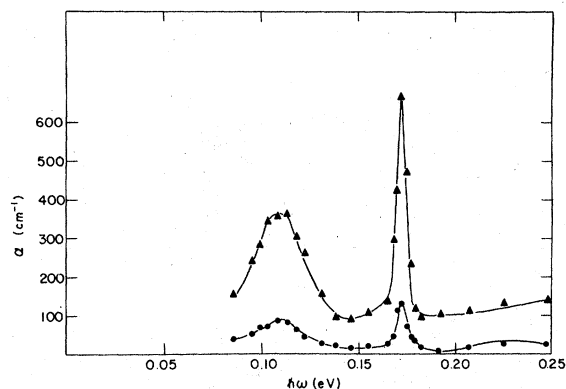


FIG. 5. Additional absorption (over the undoped sample) as a function of energy (in eV) for dilute (<0.1%) sodium in *cis*-(CH)_x (note that 900 cm⁻¹=0.11 eV and 1370 cm⁻¹=0.17 eV).

efficient of approximately $\alpha \approx 500 \text{ cm}^{-1}$ (sample thickness = 60 μm).

The microwave cavity perturbation measurements yielded a value for $\epsilon_1(10 \text{ GHz}) = 9.3$ for oriented films of (CH)_x. To obtain this number we carried out the measurements on aligned films as described in Sec. II using as the filling factor $\alpha = \frac{1}{3} V_s/V_c$, where the factor $\frac{1}{3}$ results from the relative density of the (CH)_x films. Examination of the fibrous structure of the aligned films by electron microscopy gives confidence that the depolarization factor is small ($\approx 10^{-2}$) for the electric field parallel to the orientation direction (i.e., parallel to the polymer fibrils) and large (~ 1) for the electric field perpendicular to the orientation direction. Incomplete orientation limits the accuracy;

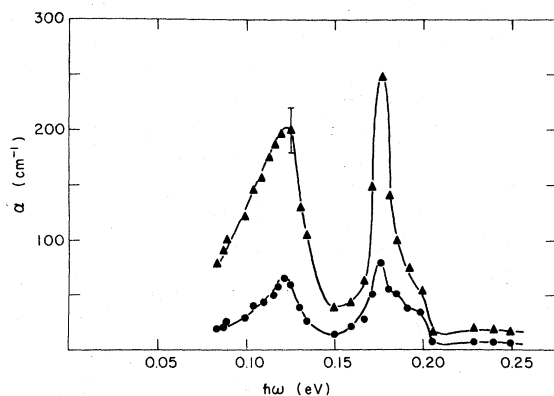


FIG. 6. Additional absorption (over the undoped sample) as a function of energy (in eV) for dilute iodine in *trans*-(CH)_x (note that 900 cm⁻¹=0.11 eV and 1370 cm⁻¹=0.17 eV). The upper curve corresponds to approximately 0.1-mole% iodine (0.03% I₃⁻), the lower curve to 0.015% (0.005% I₃⁻).

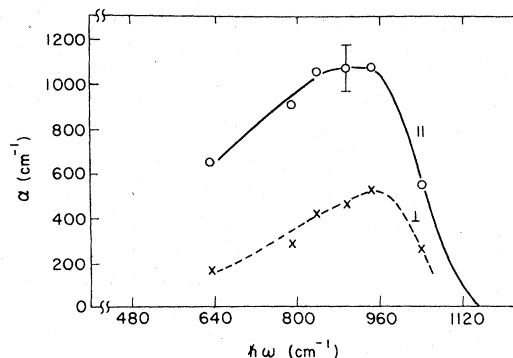


FIG. 7. Polarization dependence of the 900-cm⁻¹ ($\sim 0.11 \text{ eV}$) absorption for *cis*-(CH)_x lightly doped (<0.1%) with iodine. || and \perp refer to ir electric field polarized parallel and perpendicular to the orientation direction.

the above value is a lower limit. From a combination of the anisotropy in the optical reflectance data plus electron microscopy we estimate 70%–90% alignment in the bulk of the film, implying $\epsilon_1 \approx 10$ –12. Note that ϵ_1 in (CH)_x is expected to be anisotropic. The above value represents the value appropriate to electric fields parallel to the (CH)_x chains, $\epsilon_1^{\parallel} = 10$ –12; we currently have no measurement of ϵ_1^{\perp} .

IV. DISCUSSION

The simplest model of the donor or acceptor state follows the traditional semiconductor approach and pictures the electron or hole, with an effective mass determined by the band structure, loosely bound to the charged center by Coulomb forces in a dielectric medium.^{17,18} This model results in simple hydrogeniclike orbitals for the donor and acceptor states. The binding energy of the

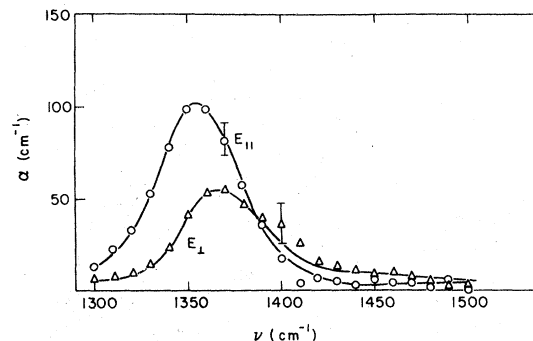


FIG. 8. Polarization dependence of the 1350-cm⁻¹ ($\sim 0.17 \text{ eV}$) absorption for *cis*-(CH)_x lightly doped (<0.1%) with iodine. || and \perp refer to ir electric field parallel and perpendicular to the orientation direction.

most tightly bound orbit with $1s$ character is

$$\epsilon_B = -(e^2/2a_0)[(m^*/m)(1/\epsilon^2)],$$

where a_0 is the Bohr radius. The radius of such an orbit is $a^* = a_0 \epsilon m/m^*$. In the case of silicon $\epsilon_B = 0.04$ eV; for germanium $\epsilon_B = 0.01$ eV. The radius of the $1s$ -like state in silicon is $a^* \approx 25$ Å. The observed small values for ϵ_B are consistent with the relatively large values obtained for the dielectric constant.

The 0.11-eV absorption described in Figs. 1-8 is a possible candidate for the ionization of the donor or acceptor states in doped $(\text{CH})_x$. The width of the mode argues against the possibility that the absorption has its origin in a molecular vibration associated with the introduction of the dopant into the polymer. More importantly it would be difficult to understand why the absorption mode should be at the same energy for several different dopant species.

In an attempt to apply the traditional approach to donor (acceptor) states in semiconductors we assume the following model for the impurity states in lightly doped $(\text{CH})_x$. Instead of substitutionally replacing the host as in silicon, the impurity resides very close to the polymer chain, either on the surface of the 200-Å fibrils and/or between individual chains. At the light doping levels studied here we assume isolated impurities interacting with a single polymer chain. At heavy doping levels impurity interactions will become important. However, at the doping levels used in the present experiments this should not be a problem.

We consider then a model system of an impurity interacting with a polymer chain as sketched schematically in Fig. 9(a). The impurity could either donate an electron to, or accept an electron from, the chain. In the donor case, the electron on the chain would be in an empty conduction band free to delocalize if it were not for the Coulomb binding to the impurity [Fig. 9(b)]. The expected absorption would correspond to the ionization of this weakly bound state. The binding energy of such an impurity state is the same as for donors and acceptors in traditional semiconductors scaled to the proper dielectric constant. The resulting localized state energy levels are in the gap as indicated in Fig. 9(c). Note that these localized states are *not* charge transfer states; the ionic species, e.g., I_3^- or Na^+ , are stable in $(\text{CH})_x$ with energy levels below the top of the valence band or above the bottom of the conduction band, respectively. The localized states of Fig. 9 are bound states of the electron or hole on the polymer chain in the vicinity of the charged donor or acceptor ion. Because the carriers are restricted to the polymer chains, in the case of weak interchain coupling, one would

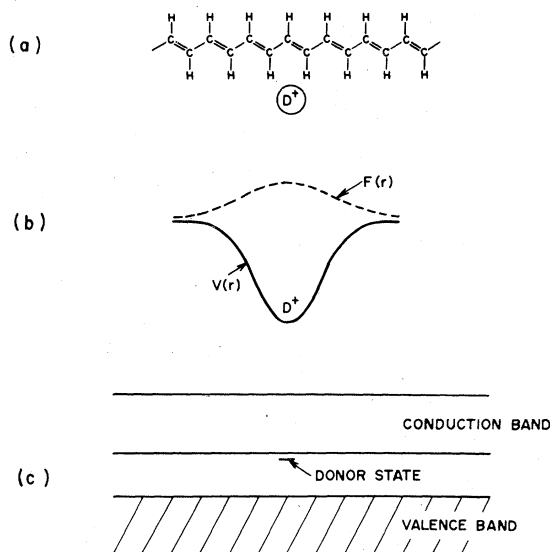


FIG. 9. (a) Schematic diagram of donor (or acceptor) ion near a $(\text{CH})_x$ chain. (b) The resulting electron (or hole) on the polymer chain is bound by the Coulomb potential [$V(r)$] to the region of the chain near the donor (or acceptor) ion. The envelope function of the wave function is $F(r)$. (c) The resulting donor (or acceptor) bound states are in the energy gap (see text).

expect to observe strong polarization effects. This qualitative picture is in general agreement with the experimental results.

Although it is somewhat surprising that a simple hydrogenic model should be applicable in this case of reduced dimensionality, the impurity states in $(\text{CH})_x$ can be treated in direct analogy to donor and/or acceptor states in conventional semiconductors.^{17,18} In the case of $(\text{CH})_x$, we approximate the polymer chain by a one-dimensional chain and use the effective-mass equations to solve for the modulation envelope of the Wannier functions in the presence of a slowly varying Coulomb potential as a perturbation. Writing

$$H\varphi_0(r) = \epsilon_B\varphi_0(r), \quad (2)$$

where

$$\varphi(r) = A \sum_n F(R_n) \chi_\pi(r - R_n) \quad (3)$$

and $\chi_\pi(r)$ is the Wannier function, A is the normalization constant, and $F(R_n)$ is the envelope function. Using the orthogonality of the Wannier functions, one obtains (in the continuum limit)

$$[(1/2m^*)p_y^2 - e^2/\epsilon_{||}|y|]F(y) = \epsilon_B F(y). \quad (4)$$

In this equation ϵ_B is the binding energy of the

electron or hole in the Coulomb field screened along the polymer chain by ϵ_{\parallel} , the dielectric constant along the chain (taken to be in the \hat{y} direction). Only the effective mass for motion along the y axis appears because we have assumed weak interchain coupling and thus approximated the transverse mass as infinite. This appears to be a reasonable assumption given the observed transport⁴ and optical⁷ anisotropies and the fact that estimates of the ratio of longitudinal to transverse bandwidths are as large as 10^2 .^{5,8} Equation (4) was simplified by ignoring the finite size of the donor or acceptor ion and assuming $(y^2 + d^2)^{1/2} \approx |y|$, where d is the perpendicular distance from the impurity to the chain. Although not exact, this approximation will not lead to serious error so long as the ion size and the distance d are small compared to the bound-state dimension as discussed below. The equation for $F(y)$ is the Schrödinger equation for a one-dimensional atom. The solutions to this problem have been discussed extensively with the important result that the spectrum of energy eigenvalues is the same as in the three-dimensional case except that only ϵ_{\parallel} is involved:

$$\epsilon_B = -(e^2/2a_0)(m^*/m\epsilon_{\parallel}^2). \quad (5)$$

The envelope function is of the form

$$F(R_n) = (|R_n|/a_0\epsilon_{\parallel}) \exp(-|R_n|/a_0\epsilon_{\parallel}). \quad (6)$$

If we take the $2p_z$ atomic orbitals for carbon as the approximate Wannier functions, the bound-state wave function [Eq. (3)] describes an electron (or hole) in the $2p_z$ orbitals of carbon atoms near the dopant impurity with a probability distribution defined by the square modulus of the envelope function [Fig. 9(b)]. Photoionization of the bound state would occur at $\hbar\omega = |\epsilon_B| = 13.6/\epsilon_{\parallel}^2$ eV assuming a free-electron effective mass along the chain. Taking the measured dielectric constant to be $\epsilon_{\parallel} = 10$ – 12 and assuming $m^*/m \approx 1$, we estimate the absorption to occur in the vicinity of 0.10–0.14 eV, polarized along the chain direction. The above analysis is clearly oversimplified. We have assumed three-dimensional screening even though the anisotropy is known to be large. Although inclusion of anisotropy will introduce numerical corrections to the screening length, it should not change the order of magnitude.

Within this simple theory, the bound-state energy would be independent of dopant (donor, acceptor, etc.) as observed experimentally. However, such a general feature is expected only if the size of the bound state, $\sim 2\epsilon_{\parallel}a_0$, is much greater than the size of the ionic impurity (e.g., I_3^- , etc.). Since $2\epsilon_{\parallel}a_0 \approx 10$ – 15 Å for $(CH)_x$, the identical absorptions observed for iodine, AsF_6 , and Na are somewhat surprising.

The strength of the absorption can be estimated from standard theory. Burstein *et al.*¹⁹ give the approximate cross section for a photoionization of the bound state near threshold energy:

$$\sigma = (8.28 \times 10^{-17} / \epsilon_B \sqrt{\epsilon_{\parallel}}) (m/m^*) (\epsilon_B / \hbar\omega)^{8/3}, \quad (7)$$

where ϵ_B is in eV. Since $\alpha = \sigma n$, where n is the concentration of impurity centers, the estimated absorption coefficient for $n = 0.1\%$ is $\alpha \approx 5.4 \times 10^3$ cm^{-1} . The measured value of the peak absorption observed in the polarized data (Fig. 7) is approximately an order of magnitude smaller. In addition, the shape of the absorption curve is not typical of a photoionization process where one expects a relatively sharp onset with a slower falloff at higher energies. However, local variations in the polymer, for example in ϵ_{\parallel} , due to incomplete orientation and only partial crystallinity would tend to smear the shape and decrease the peak amplitude of absorption.

From such a picture, the semiconductor-metal transition can be understood. Starting from the metallic (high-concentration) side, a decrease in concentration of impurities results in a decrease in the number of available charge carriers; thus there are fewer carriers available to screen the impurity potential. In the Thomas-Fermi approximation the screening length

$$\lambda = (4m^*e^2n^{1/3} / \epsilon_{\parallel}\hbar^2)^{-1/2},$$

where we have assumed the medium to have a dielectric constant equal to ϵ_{\parallel} , appropriate to the chain axis; n is the electron density and m^* is the electron effective mass. When the screening length has grown larger than the adjusted Bohr radius, it becomes energetically favorable for the ionized holes or electrons to form bound states with the charged centers. This further decreases the carrier concentration while increasing the binding energy of the electron or hole to an impurity. The result is a transition from delocalized to localized states: a metal-to-semiconductor transition.^{20,21} There have also been attempts to describe the transition from the semiconducting side by use of the Hubbard model.²² As the concentration of impurities increases, the expanded wave functions of the hole or electron begin to overlap with those on nearby sites, thus increasing the transfer integral t . At high enough concentrations, the dimensionless quantity t/U grows larger than the critical value needed for formation of delocalized bandlike states (U is the on-site Coulomb interaction) for the impurity electrons or holes. Numerical studies indicate that the critical concentration depends upon the choice of the coefficient γ , where the criterion for metallic behavior is $\gamma(t/U) > 1$, but the results are relatively insensitive

to γ . For example Berggren²³ has shown that t/U increases rather slowly with concentration until the critical region where it grows rapidly. Thus the critical concentration depends only weakly on γ .

Both the Thomas-Fermi approximation and the Hubbard model lead to the rather general statement known as the Mott criterion for the critical concentration for the semiconductor-metal transition²⁴:

$$\eta_c^{1/3} = (4a_0)^{-1}(m^*/m\epsilon). \quad (8)$$

This model has been used in the initial discussion of the semiconductor-metal transition in $(\text{CH})_x$.³ However, prior to the data presented in this paper there has been no experimental evidence of extended hydrogenic orbits for impurity states in $(\text{CH})_x$. Using Eq. (8), with $\epsilon_{\parallel} \approx 10$ and $m^*/m \sim 1$, we estimate $\eta_c \approx 10^{20} \text{ cm}^{-3}$, in reasonable agreement with the experimental value.³

In summary the simple hydrogenic model for the isolated donor/acceptor states is only partially successful in accounting for the experimental observations. The calculated binding energy is in good agreement, and the theory based on this approach gives a correct estimate of the critical concentration at the semiconductor-metal transition. However, the shape and intensity of the absorption are quite far off. Moreover, the remarkable quantitative insensitivity of the energies of the absorption maxima to the dopant species is difficult to understand within a realistic application of the model. Finally, the intense, narrow, molecular-like, absorption at 1370 cm^{-1} cannot be understood within this model.

The analysis presented above assumes a rigid

band structure along the lines of traditional semiconductor physics. However, the bond-alternation energy gap in polyacetylene may be viewed as the result of the $2k_F$ instability in a quasi-one-dimensional metal.^{25,26} In this point of view,²⁷ the effect of charge-transfer doping would be to change $k_F = (\pi/2)n$, where n is the number of carriers per unit length along the chain in the undistorted metallic state. In the pure polymer, there is one π electron per carbon atom corresponding to a half-filled band so that $n_0 = a^{-1}$, where a is the uniform carbon-carbon bond length and $k_F = k_F^0 = \pi/2a$. The resulting charge-density-wave distortion occurs with a superlattice period $b_s^0 = 2\pi/2k_F = 2a$, implying a dimerized bond-alternating structure as observed in $(\text{CH})_x$. Doping will change k_F ; $k_F = (\pi/2)n_0(1 \pm c)$, where c is the impurity concentration, and the plus or minus sign is appropriate for donor or acceptor doping. We have assumed complete charge transfer. The resulting superlattice period will shift away from $b_s^0 = 2a$ to a new value $b_s = 2a/(1 \pm c)$, incommensurate with the carbon-chain polymer structure. However, the commensurability energy strongly favors locking $2k_F$ at the zone boundary; a commensurate bond alternation with period $2a$ places π -bond charge between carbon atoms [Fig. 10(a)], whereas in the incommensurate case, the charge-density maxima and minima would not be related to the atomic positions.

The commensurate-incommensurate phase transition in the presence of a large commensurability potential has been a subject of considerable theoretical interest in recent years.²⁸⁻³⁰ It is found²⁸⁻³⁰ that for small deviations from the half-filled band case (i.e., for small concentrations c) the solution

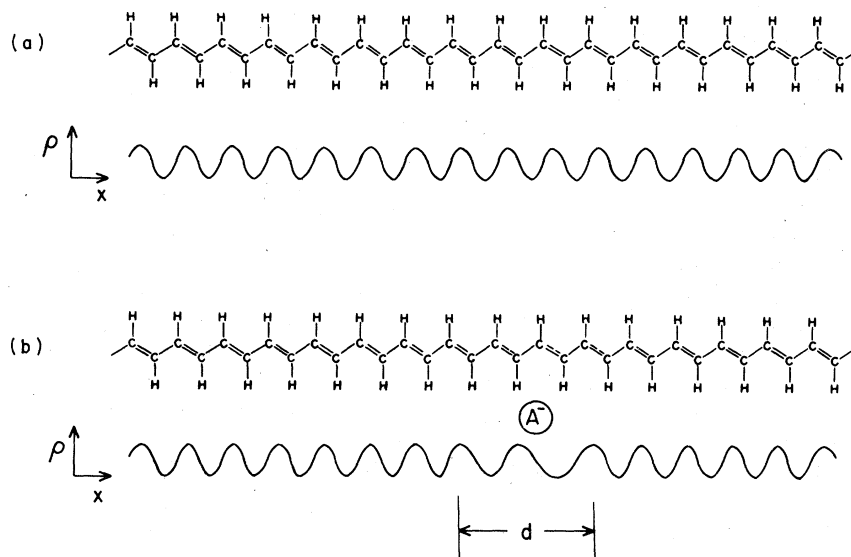


FIG. 10. (a) Schematic diagram of bond-alternated polyene. The π charge density $\rho(x)$ is plotted below, showing the buildup and depletion of bond charge between successive neighbors. (b) Schematic diagram of bond-alternated polyene with a 2π phase-kink distortion caused by charge transfer to nearby acceptor. The missing π bond is arbitrarily spread over three lattice constants for illustration, i.e., the domain-wall thickness d is chosen as three lattice constants. In general there may be both an amplitude distortion and a phase distortion within the wall.

consists of relatively large domains in which $k_F = k_F^0 = \pi/2a$ separated by localized domain-wall-like regions. Within the domain walls, the charge-density wave is incommensurate; the phase is stretched or contracted such that either one full period (2π) or one half period (π) is added or subtracted within the width of the wall. Since each full period or each 2π of phase in the charge-density wave corresponds to a charge of $2e$, the domain wall is charged with $q=2e$ (2π phase kink) or $q=e$ (π phase kink). Both the overall periodicity and the average charge density are preserved. Phase distortions will exist without associated amplitude distortions provided the mean-field transition temperature is high and the order parameter is well developed. In general, one can expect, in addition, some reduction in amplitude within the wall.

This phase-kink doping has a simple chemical interpretation. Consider first the 2π phase kink as sketched in Fig. 10(b). Acceptor doping would result in localized domain-wall-like positively charged regions, in which two π electrons, in effect, one π bond, would be removed and the charge transferred to nearby acceptor impurities. The result would be a 2π phase kink distributed over a group of carbon atoms in the domain wall along the polymer chain. Although similar to the phase-soliton excitations³¹ of the charge-density-wave (CDW) condensate, these localized distortions would be a property of the ground state of the doped polymer, induced so that the perturbed bond-alternation charge-density wave can continue to take advantage of the large commensurability energy. The π phase kink separates regions in which alternating double and single bonds are shifted by one carbon-carbon bond length (i.e., single-double-single-double, etc., on the left, and double-single-double-single, etc., on the right). For the π kink, the resulting unpaired electron on the central carbon is transferred to a nearby acceptor and the resulting positive charge is delocalized over the width of the wall. Such charged regions would be bound to the dopant impurity by the Coulomb interaction resulting in a polarized ionization absorption similar to that described above. An estimate of the binding energy would require knowledge of the charge, e or $2e$, and the effective mass M (currently unknown) of the phase-kink domain wall.

This type of ground state might also provide a source for the strong absorption observed in the infrared at 1370 cm^{-1} . Within the region of the "phase kink," the charge-density wave would be incommensurate with the underlying polymer im-

plying an average bond order close to 1.5. It is therefore tempting to suggest that the 1370-cm^{-1} mode, which occurs at a frequency approximately intermediate between a single-bond (C-C; $\sim 950\text{ cm}^{-1}$) and double bond (C=C; $\sim 1650\text{ cm}^{-1}$) vibration corresponds to a region of uniform bond lengths characteristic of the uniform polyene chain. Although a detailed theory is not yet available, the locally incommensurate charge-density wave breaks the inversion symmetry so that carbon-carbon stretching modes could become ir active. The intensity of the observed absorption implies an enhanced oscillator strength with a substantial electronic contribution perhaps resulting from a combination of wall motion and molecular vibration in response to the oscillating electric field of the ir wave (wall motion can lead to an enhanced effective oscillating ir electric field in a manner analogous to the radio frequency magnetic field enhancement observed in nuclear-magnetic-resonance absorption in the domain walls of ferromagnets³²). The induced ir activity would thus be somewhat similar to that proposed by Rice^{33,34} in studies of the coupling of symmetric molecular vibrations to charge-density waves. Detailed calculations are required for quantitative comparison with experiment.

V. SUMMARY AND CONCLUSION

In summary, we have shown that the impurity states in polyacetylene can be analyzed in a manner quite analogous to that used in the traditional semiconductors. However, viewing $(\text{CH})_x$ as a one-dimensional metal driven to bond alternation by the Peierls instability leads to a new type of donor (acceptor) state similar to the phase soliton excitations of the charge-density-wave condensate. The experimental ir absorption changes observed upon doping are discussed in the context of these models of the doping in this conjugated polymer.

ACKNOWLEDGMENTS

We thank Dr. M. J. Rice for suggesting the possibility of doping through phase distortions in a quasi-one-dimensional semiconductor. Several stimulating conversations with Professor J. R. Schrieffer were helpful in clarifying the physics of the π and 2π phase kinks. Discussions with Professor E. Burstein on the applicability of traditional semiconductor physics to the doping of these polymer systems were extremely useful. Work has been supported by the office of Naval Research.

- *Permanent address: Asahi Chemical Industry, 2-1, Samejima, Fuji-shi 1416, Shizuoka-Ken, Japan.
- ¹H. Shirakawa, E. J. Louis, A. G. MacDiarmid, C. K. Chiang, and A. J. Heeger, *Chem. Commun.* **578** (1978).
- ²C. K. Chiang, M. A. Druy, S. C. Gau, A. J. Heeger, H. Shirakawa, E. J. Louis, A. G. MacDiarmid, and Y. W. Park, *J. Am. Chem. Soc.* **100**, 1013 (1978).
- ³C. K. Chiang, C. R. Fincher, Jr., Y. W. Park, A. J. Heeger, H. Shirakawa, E. J. Louis, S. C. Gau, and A. G. MacDiarmid, *Phys. Rev. Lett.* **39**, 1098 (1977).
- ⁴Y. W. Park, M. A. Druy, C. K. Chiang, A. J. Heeger, A. G. MacDiarmid, H. Shirakawa, and S. Ikeda, *Polym. Lett.* **17**, 195 (1979).
- ⁵C. K. Chiang, Y. W. Park, A. J. Heeger, H. Shirakawa, E. J. Louis, and A. G. MacDiarmid, *J. Chem. Phys.* **69**, 5098 (1978).
- ⁶C. K. Chiang, S. C. Gau, C. R. Fincher, Jr., Y. W. Park, A. G. MacDiarmid, and A. J. Heeger, *Appl. Phys. Lett.* **33**, 181 (1978).
- ⁷C. R. Fincher, Jr., D. L. Peebles, A. J. Heeger, M. A. Druy, Y. Matsumura, and A. G. MacDiarmid, *Solid State Commun.* **27**, 489 (1978).
- ⁸P. M. Grant and I. P. Batra, *Solid State Commun.* (to be published); P. M. Grant, *Bull. Am. Phys. Soc.* **23**, 305 (1978).
- ⁹S. Hsu, A. Signorelli, G. Pez and R. Baughman, *J. Chem. Phys.* **68**, 5405 (1978); **69**, 106 (1978).
- ¹⁰H. Shirakawa, T. Sasaki, and S. Ikeda (unpublished).
- ¹¹C. R. Fincher, Jr., Y. Matsumura, A. J. Heeger, and A. G. MacDiarmid, *Bull. Am. Phys. Soc.* **23**, 304 (1978).
- ¹²H. Shirakawa and S. Ikeda (unpublished).
- ¹³H. Shirakawa and S. Ikeda, *Polym. J.* **2**, 231 (1971); H. Shirakawa, T. Ito, and S. Ikeda, *ibid.* **4**, 460 (1973); T. Ito, H. Shirakawa, and S. Ikeda, *J. Polym. Sci. Polym. Chem. Ed.* **12**, 11 (1974); 1943 (1975); H. Shirakawa, T. Ito, and S. Ikeda, *Die Macromoleculare Chemie* **179**, 1565 (1978).
- ¹⁴M. A. Druy, N. Brown, and A. G. MacDiarmid (unpublished).
- ¹⁵L. I. Buravov and I. F. Shchegolev, *Prib. Tekh. Eksp.* **2**, 171 (1971).
- ¹⁶S. K. Khanna, E. Ehrenfreund, A. F. Garito, and A. J. Heeger, *Phys. Rev. B* **10**, 2205 (1974).
- ¹⁷W. Kohn and J. M. Luttinger, *Phys. Rev.* **98**, 915 (1955); W. Kohn, *Solid State Physics*, Vol. 5, edited by F. Seitz and D. Turnbull (Academic, New York, 1958).
- ¹⁸C. Kittel and A. H. Mitchell, *Phys. Rev.* **96**, 1488 (1956).
- ¹⁹E. Burstein, G. Picus, B. Henvis, and R. Wallis, *J. Phys. Chem. Solids* **1**, 75 (1956).
- ²⁰N. F. Mott, *Metal-Insulator Transitions* (Taylor and Francis, London, 1974).
- ²¹N. F. Mott, *Proc. Phys. Soc.* **62**, 416 (1949).
- ²²J. Hubbard, *Proc. R. Soc. A* **276**, 238 (1963); **277**, 237 (1963); **281**, 401 (1964).
- ²³K. Berggren, *Philos. Mag.* **27**, 1027 (1973).
- ²⁴P. Edwards and M. Siekno, *Phys. Rev. B* **17**, 2575 (1978).
- ²⁵*Low Dimensional Cooperative Phenomena*, edited by H. J. Keller (Plenum, New York, 1975); *Chemistry and Physics of One Dimensional Metals*, edited by H. J. Keller (Plenum, New York, 1977).
- ²⁶*One Dimensional Conductors*, edited by J. Devreese (Plenum, New York, 1978).
- ²⁷M. J. Rice (private communication).
- ²⁸W. L. McMillan, *Phys. Rev. B* **14**, 1496 (1976).
- ²⁹P. Bak (unpublished).
- ³⁰L. Bulaevskii (unpublished).
- ³¹M. J. Rice, A. R. Bishop, J. A. Krumhansl, and S. E. Trullinger, *Phys. Rev. Lett.* **36**, 432 (1976).
- ³²A. M. Portis and R. H. Lindquist, *Magnetism*, Vol. II, edited by H. Suhl and G. Rado (Academic, New York, 1963).
- ³³M. J. Rice, *Phys. Rev.* **37**, 36 (1976).
- ³⁴M. J. Rice, N. O. Lipari, and S. Strässler, *Phys. Rev. Lett.* **39**, 1359 (1977).